Proceedings of the 6th International Conference on Energy Harvesting, Storage, and Transfer (EHST'22)
Niagara Falls, Canada – June 08-10, 2022
Paper No. 138
DOI: 10.11159/ehst22.138

Investigating Phase Change Material Foam Configuration in a Heat Exchanger

Kasra Ghasemi[1], Mohammad Reza Mohaghegh[1], Mehran Bozorgi [1], Syeda Tasnim[1], Shohel Mahmud[1]
[1]School of Engineering, University of Guelph, Guelph, Ontario, Canada
kghasemi@uoguelph.ca; mohaghem@uoguelph.ca; mbozorgi@uoguelph.ca; stasnim@uoguelph.ca; smahmud@uoguelph.ca

Abstract **-** Phase change material can be used in a heat exchanger to smooth out the temperature during cyclic or pulsed operations. However, the performance is highly dependent on the design and thermophysical properties of embedded PCM. In this study, the effects of location and amount of embedded PCM on the melting time in a shell and tube heat exchanger are evaluated by developing a Lattice Boltzmann Method code. The PCM is encapsulated in circular metal foam surrounding the inner tube using hot water as the working fluid. According to the results, inner tube location has a significant effect on the natural convection, and consequently, the melting time and rate. It is observed that placing the inner tube near to the downside of the PCM layer, causes a more uniform temperature distribution within the domain and has the lowest melting time. Also, while increasing the thickness of the PCM layer enhances the melting time, this increment has an exponential relation with the melting time.
Keywords**:** Phase Change Material, Heat Exchanger, Metal Foam, Melting Performance, Lattice Boltzmann Method;

1. Introduction

Phase change material (PCM) is working based on the phase transition concept, usually solid to liquid and vice versa, in thermal energy storage (TES). The energy stored and released by PCM during the melting and solidification processes, respectively, is at least 1-2 orders of magnitude higher than the energy stored by the specific heat in sensible TES [1], [2]. So, these materials are suitable for thermal management such as smoothing out the peak load, short-term energy storage, and protection from failure during coolant interruptions. PCM in a heat exchanger can play a significant role in reducing energy consumption and implementing a lower capacity pump for a certain application. Shell and tube, double pipe and plate heat exchangers are the most common models using PCM for different substantial applications, including pulsed electronics [3], HVAC [4], solar systems [5], and condensers in refrigeration cycles [6].

Although the concept has high potential in energy management, it must be analyzed and optimized from various aspects to reduce costs and increase efficiency. So far, many researchers are attracted to the subject and several studies are conducted in the last two decades in terms of physical and thermal characteristic features [7]. One of the main disadvantages of PCM is their low thermal conductivity which results in low heat transfer. To overcome this issue, Mahdi et al. [8] introduced a hybrid approach by implementing fin-assisted metal foam strips around a tube. They demonstrated that the thermal response of the PCM layer enhances considerably by this new model. The evaluation is performed for both solidification and melting processes, and up to 58.42% improvement is reported. In another study on a shell and tube heat exchanger, Mahdi and Nsofor [9] investigated the influences of the porous foam containing PCM on the heat absorption performance. According to their results, embedding cascaded metal foam with high porosity in the heat flow direction can compensate for the low thermal conductivity of PCM.

PCM is a relatively expensive material, and also, adding PCM into a heat exchanger requires space. So, the amount and design of the PCM layer are of great importance that need to be optimized. One of the interesting studies on PCM configuration is conducted by Vyshak and Jilani [10]. In this research, three shapes of PCM as planar, inner, and outer layers are compared that have the same amount of PCM and contact surface area. Their results revealed that cylindrical shell PCM takes the least time for storing equal amounts of energy. It is also observed that increasing the inlet temperature of heat transfer fluid (HTF) drastically reduces the energy storage time in cylindrical shell PCM compared to other models. Later, Esapour et al. [11] investigated the effects of orientation and number of tubes on the melting time in multi-tube storage systems. They claimed that by approaching the inner tubes to the bottom of the shell the melting process accelerates. Also, increasing the number of tubes results in a higher contact area between PCM and HTF, thus lower melting time and a higher heat transfer achieves.

The type of used PCM and properties of HTF have also demonstrated a significant impact on the efficiency and melting performance [12]. Pahamli et al. [13] studied the melting performance of PCM in a horizontal double pipe heat exchanger. They reported that the downward movement of the inner tube strengthens the convection, and consequently, reduces melting time up to 64%. They also indicated that rising inlet temperate on HTF has a direct relation with a decrement in the melting time. On the other hand, the increment in the mass flow rate does not show a considerable impact on the melting performance. Putra et al. [14] researched the passive cooling of a heat pipe by using PCM in an electrical device. They focused on determining the effectiveness of the cooling system and identifying the optimal PCM. It is stated that the PCM type must be selected according to the application and the temperature range of the HTF. In other words, the melting point of PCM is of great importance in the efficiency of the system, especially for small-scale applications.

Based on the reviewed literature, it is observed that the performance of PCM in a heat exchanger depends on several characteristic parameters, especially configuration, that demand further investigations. In this study, the effects of inner tube location and PCM layer thickness are evaluated to reach a better efficiency in terms of melting rate. The PCM is embedded in a metal foam with high thermal conductivity and porosity. This numerical research is conducted by developing a Lattice Boltzmann Method code in FORTRAN software.

2. Methodology

In this section, the considered problem is described for input parameters, the governing equations are presented and the numerical model for the simulations is reported.

2.1. Problem Description

A schematic of the circular sectional area of a shell and tube heat exchanger is demonstrated in Fig. 1. The shell is filled with n-octadecane PCM embedded in a metal foam with thermophysical properties given in Table 1. The inner tube's location, d(x, y), and thickness of the shell (t) are variables given in Table 2. The parameter |d|, diameter and temprature of the inner tube are set to 0.01 m, 0.02 m and 31 ℃, respectively. The Newtonian fluid and incompressible assumptions are applied for the natural convection within the liquid phase. For the given dimensions and PCM properties, the fluid flow is within the laminar regime. Also, a regular shape porous foam is assumed, and the Brinkman-Forchheimer model is applied for the REV modelling with porosity (ε) and thermal conductivity of 0.9 and 100 W/m.K, respectively.

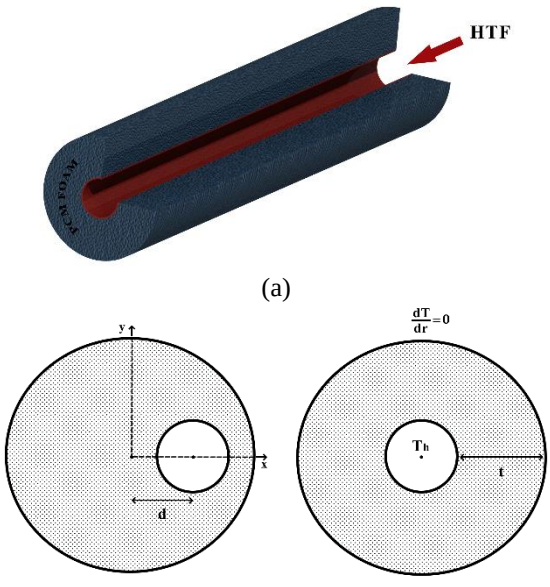

Fig. 1: Schematic of the problem in (a) 3D, and (b) 2D forms.

Table 1: Thermophysical properties of n-octadecane [15].

	ρ (kg/m^3)	c_p (J/kg.K)	k (W/m.K)	β (1/K)	υ (m^2/s)	L (kJ/kg)	T_m (℃)
PCM	770	2300	0.15	0.001	5×10^{-6}	243	30

Table 2: Considered values for tube location and PCM layer thickness.

	1	**2**	**3**	**4**
d(x, y)	(0, 0)	(d, 0)	(d, 0)	(0, -d)
t (m)	0.005	0.01	0.015	0.02

2.2. Governing Equations

For the described problem in section 2.1, the dimensionless governing equations, including continuity, momentum and energy, are [16]:

$$\nabla.\vec{U} = 0 \tag{1}$$

$$\frac{\partial \vec{U}}{\partial t} + \left(\vec{U}.\nabla\right)\left(\frac{\vec{U}}{\varepsilon}\right) = -\frac{1}{\rho_{PCM}}\nabla(\varepsilon p) + \nu_{PCM}\nabla^2\vec{U} - \frac{\varepsilon\nu_{PCM}}{K}\vec{U} - \frac{\varepsilon F_\varepsilon}{\sqrt{K}}\left|\vec{U}\right|\vec{U} - \varepsilon\vec{g}\beta_{PCM}(T - T_{ave}) \tag{2}$$

$$\sigma\frac{\partial T}{\partial t} + \vec{U}.\nabla T = \nabla.\left(\frac{k_e}{(\rho c_p)_{PCM}}\nabla T\right) - \varepsilon\frac{L_{sl}}{c_{p_{PCM}}}\frac{\partial f_l}{\partial t} \tag{3}$$

Where K, σ, L_{sl} and f_l are permeability, thermal capacity ratio, latent heat and liquid fraction, respectively. Average temperature ($T_{ave} = \frac{T_h + T_i}{2}$), geometry function ($F_\varepsilon = \frac{1.75}{\sqrt{150\varepsilon^3}}$) and effective thermal conductivity ($k_e = \varepsilon k_{PCM} + [1-\varepsilon]k_p$) are calculated accordingly.

The melting fraction of PCM is calculated by using enthalpy (H) definition as:

$$f_l = \begin{cases} 0 & H < H_s \\ \frac{H - H_s}{H_l - H_s} & H_s \le H \le H_l \\ 1 & H_l < H \end{cases} \tag{4}$$

Where $H = c_p T + L f_l$. Detailed information for this section's equations is provided in [17].

2.3. Lattice Boltzmann Method

An in-house Lattice Boltzmann Method (LBM) code is written to solve the governing equations. The flow part has a moving boundary, and so, its effects are added to the collision step based on the BGK approximate. Also, for the thermal field, the model introduced by Huang et al. [18] is applied which calculates enthalpy instead of temperature in the distribution functions. The followings are applied for the calculations by using a D2Q9 lattice [19], [20]:

$$f_i(x + c_i\Delta t, t + \Delta t) - f_i(x,t) = -\frac{1-B}{\tau_f}\left[f_i(x,t) - f_i^{(eq)}(x,t)\right] + B\Omega_i^s + \Delta t.F_i \tag{5}$$

$$g_i(x + c_i\Delta t, t + \Delta t) - g_i(x,t) = -\frac{g_i(x,t) - g_i^{(eq)}(x,t)}{\tau_g} \tag{6}$$

Where F_i represents the body forces, and τ_f and τ_g are flow and thermal fields relations times, respectively.

The equilibrium distribution function in a thermal field is defined for latent heat calculations as:

$$g_i^{(eq)} = \begin{cases} H - c_p T + \omega_i c_p T \left(1 - \frac{\vec{U}^2}{2c_s^2}\right) & i = 0 \\ \omega_i c_p T \left[1 + \frac{\vec{c}_i.\vec{U}}{c_s^2} + \frac{\vec{U}\vec{U}:(\vec{c}_i\vec{c}_i - c_s^2 I)}{2\varepsilon c_s^4}\right] & i \neq 0 \end{cases} \quad (7)$$

In which ω_i, $\vec{c}_i$ and c_s are weighting factor, lattice speed, and sound speed, respectively. Detailed information for this section's equations is provided in [18].

3. Results and Discussion

3.1. Validation

The developed LBM code for latent heat simulation is validated by the work done by Bertrand et al. [21]. Fig. 2 presents a liquid fraction variation over time for $Pr = 0.02$, $St = 0.01$, and $Ra = 2.5 \times 10^5$ in a circular enclosure. The results are in a great match with each other.

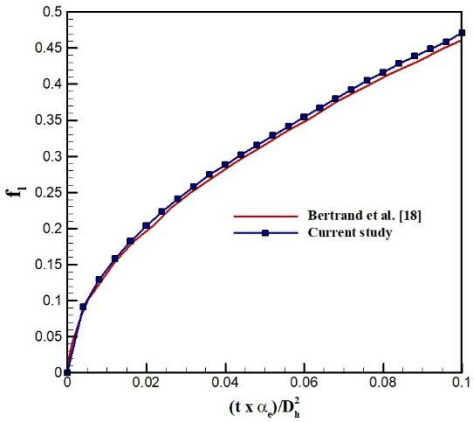

Fig. 2: Comparison for a liquid fraction in the circular domain between the current study and Bertrand et al. [21] research.

3.2. PCM Foam Configuration

In this section, the effects of the inner tube's location and PCM layer thickness on the melting time are evaluated. Firstly, isotherms within the domain for different tube locations are presented in Fig. 3 after 30 minutes of melting. It can be seen that the heat penetration is higher in d1 compared to others. In d1, d2, and d3, the heat transfer is higher in the upper region of the PCM-based foam due to the natural convection impact. However, d4 has a more uniform temperature distribution since the conduction is dominant.

In Fig. 4, the melted fraction and streamlines within the liquid part are demonstrated at the time of 30 minutes from the start of melting. It is obvious that the melting performance is higher in d1, d4, d2, and d3, respectively. A weak flow circulation in d3 has made it the worst possible location for the inner tube. Also, more powerful circulation is achieved in d4 compared to d1 which results in a higher melting rate. On the other hand, in d3 a non-uniform circulation is observable that will produce a better melting rate at the upper region, while causing a smaller heat propagation at the downward area.

To have a better undertaking of the inner tube's location impact on the melting performance, the variation of the PCM liquid fraction within the porous metal foam is reported across time in Fig. 5-a. The melting time is provided from the start until the whole PCM becomes in the liquid state. As expected from Fig. 3 and Fig. 4, d3 has the longest melting time compared to the others. This is almost twice the melting time of d1 and d4, which is considerably a high time that only has happened by changing the place of the inner tube. It shows the importance of finding the optimum location for placing the PCM layer around the hot or cold HTF for cooling and heating purposes, respectively.

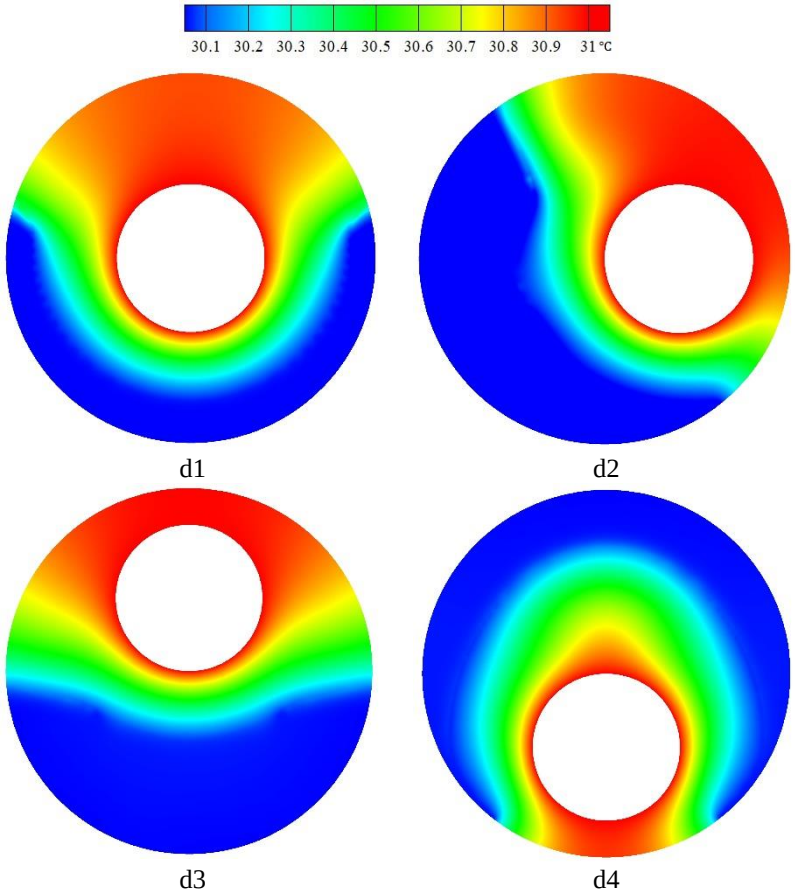

Fig. 3: Temperature distribution within the porous foam layer for different inner tube locations.

The other interesting point here is the variation of d4 along the time. While, other cases has shown reduction in the melting rate as time goes by, the melting rate of d4 stays almost constant from 10 minutes after start of melting process. As the result of this, it has obtained the lowest melting time that has made it best possible location for inner tube.

Increasing the thickness of the PCM layer obviously will enhance the melting time. But with the help of Fig. 5-b, a better understanding of the amount of this increment will be achieved. Comparing the thicknesses of t1 (smallest) and t4 (largest) demonstrates a huge difference in the melting time (around 90 minutes). The amount of added PCM to t1 is $\pi((t2+0.01)^2-(t1+0.01)^2)=0.00212\ m^2$ which means $0.02597\ m^2$ is melted in 90 minutes. On the other hand, this amount for t1 compared to t2 is $0.00055\ m^2$ in 15 minutes. So, while the ratio of added PCM region is in these two cases is proportional to 3.8545, the increased melting time ratio is 6. That means a melting time does not have a linear behavior with PCM volume.

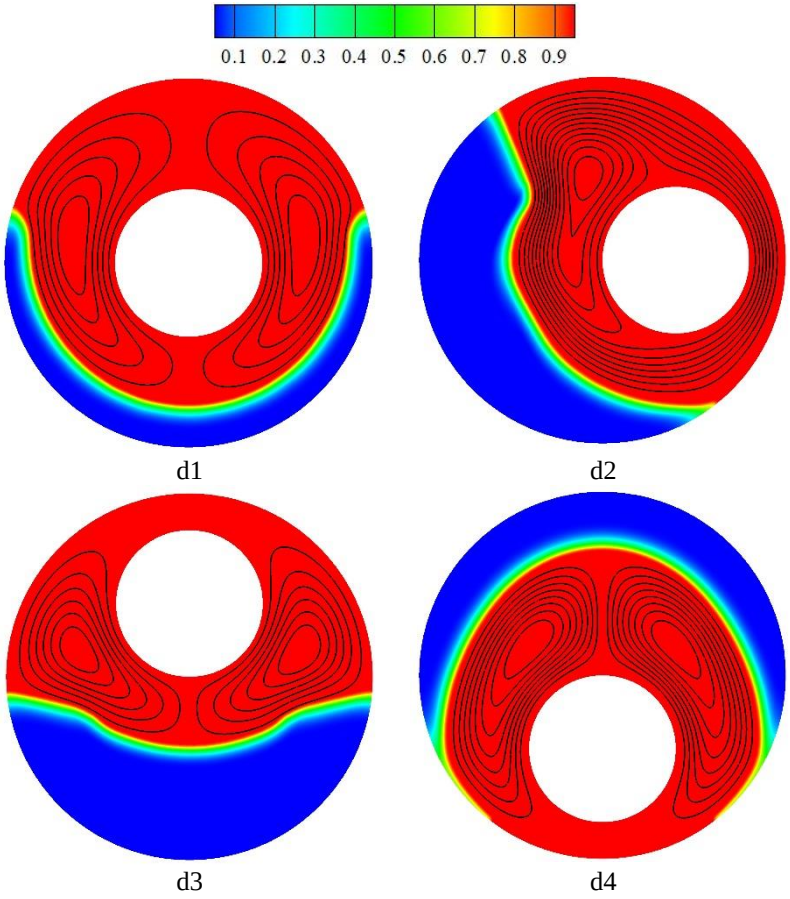

Fig. 4: liquid fraction and streamlines within the porous foam layer for different inner tube locations.

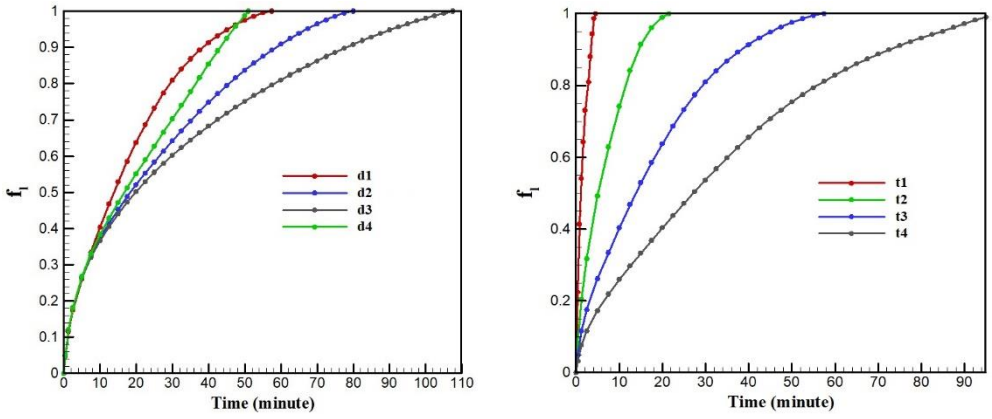

(a) (b)

Fig. 5: Liquid fraction variation over time for (a) different tube locations, (b) different PCM layer thicknesses.

4. Conclusion

In this research, the effects of PCM configuration in a shell and tube heat exchanger are investigated by using an LBM code. The PCM is embedded in a metal foam with high thermal conductivity and specific characteristic features. Two characteristic parameters, named d and t, as representatives for the location of the inner tube and thickness of PCM foam, respectively, are considered. It is observed that the location of the inner tube has significantly affected the melting time. Also, putting the inner tube near the downside of the PCM foam results in a lower melting time with an almost constant rate. Meanwhile, increasing the volume of the PCM layer does not have a linear relation with enhancement in the melting time. So, depending on the application an optimum thickness must be calculated.

Acknowledgements

The authors would appreciate the financial support provided by the Ontario Ministry of Agriculture, Food and Rural Affairs (OMAFRA) under the UG-HQP-2020-100600 Award.

References

[1] K. Ghasemi, S. Tasnim, and S. Mahmud, "PCM, nano/microencapsulation and slurries: A review of fundamentals, categories, fabrication, numerical models and applications," *Sustainable Energy Technologies and Assessments*, vol. 52, p. 102084, Aug. 2022.

[2] M. R. Mohaghegh, Y. Alomair, M. Alomair, S. H. Tasnim, S. Mahmud, and H. Abdullah, "Melting of PCM inside a novel encapsulation design for thermal energy storage system," *Energy Conversion and Management: X*, vol. 11, p. 100098, Sep. 2021.

[3] W. G. Alshaer, M. A. Rady, S. A. Nada, E. Palomo Del Barrio, and A. Sommier, "An experimental investigation of using carbon foam–PCM–MWCNTs composite materials for thermal management of electronic devices under pulsed power modes," *Heat Mass Transfer*, vol. 53, no. 2, pp. 569–579, Feb. 2017.

[4] A. Maccarini, G. Hultmark, N. C. Bergsøe, and A. Afshari, "Free cooling potential of a PCM-based heat exchanger coupled with a novel HVAC system for simultaneous heating and cooling of buildings," *Sustainable Cities and Society*, vol. 42, pp. 384–395, Oct. 2018.

[5] M. Al-harahsheh, M. Abu-Arabi, H. Mousa, and Z. Alzghoul, "Solar desalination using solar still enhanced by external solar collector and PCM," *Applied Thermal Engineering*, vol. 128, pp. 1030–1040, Jan. 2018.

[6] S. Bista, S. E. Hosseini, E. Owens, and G. Phillips, "Performance improvement and energy consumption reduction in refrigeration systems using phase change material (PCM)," *Applied Thermal Engineering*, vol. 142, pp. 723–735, Sep. 2018.

[7] M. R. Mohaghegh, S. Mahmud, and S. Tasnim, "Effect of Geometric Configurations on the Thermal Performance Of Encapsulated PCMs," presented at the ASME 2021 Heat Transfer Summer Conference collocated with the ASME 2021 15th International Conference on Energy Sustainability, Jul. 2021.

[8] J. M. Mahdi *et al.*, "Intensifying the thermal response of PCM via fin-assisted foam strips in the shell-and-tube heat storage system," *Journal of Energy Storage*, vol. 45, p. 103733, Jan. 2022.

[9] J. M. Mahdi and E. C. Nsofor, "Multiple-segment metal foam application in the shell-and-tube PCM thermal energy storage system," *Journal of Energy Storage*, vol. 20, pp. 529–541, Dec. 2018.

[10] N. R. Vyshak and G. Jilani, "Numerical analysis of latent heat thermal energy storage system," *Energy Conversion and Management*, vol. 48, no. 7, pp. 2161–2168, Jul. 2007.

[11] M. Esapour, M. J. Hosseini, A. A. Ranjbar, and R. Bahrampoury, "Numerical study on geometrical specifications and operational parameters of multi-tube heat storage systems," *Applied Thermal Engineering*, vol. 109, pp. 351–363, Oct. 2016.

[12] K. Ghasemi, S. Tasnim, and S. Mahmud, "Shape-stabilized phase change material convective melting by considering porous configuration effects," *Journal of Molecular Liquids*, vol. 355, p. 118956, Jun. 2022.

[13] Y. Pahamli, M. J. Hosseini, A. A. Ranjbar, and R. Bahrampoury, "Inner pipe downward movement effect on melting of PCM in a double pipe heat exchanger," *Applied Mathematics and Computation*, vol. 316, pp. 30–42, Jan. 2018.

[14] N. Putra, A. F. Sandi, B. Ariantara, N. Abdullah, and T. M. Indra Mahlia, "Performance of beeswax phase change material (PCM) and heat pipe as passive battery cooling system for electric vehicles," *Case Studies in Thermal Engineering*, vol. 21, p. 100655, Oct. 2020.
[15] Q. Lin, S. Wang, Z. Ma, J. Wang, and T. Zhang, "Lattice Boltzmann simulation of flow and heat transfer evolution inside encapsulated phase change materials due to natural convection melting," *Chemical Engineering Science*, vol. 189, pp. 154–164, Nov. 2018.
[16] K. Ghasemi and M. Siavashi, "Lattice Boltzmann numerical simulation and entropy generation analysis of natural convection of nanofluid in a porous cavity with different linear temperature distributions on side walls," *Journal of Molecular Liquids*, vol. 233, pp. 415–430, May 2017.
[17] K. Ghasemi and M. Siavashi, "MHD nanofluid free convection and entropy generation in porous enclosures with different conductivity ratios," *Journal of Magnetism and Magnetic Materials*, vol. 442, pp. 474–490, Nov. 2017.
[18] R. Huang, H. Wu, and P. Cheng, "A new lattice Boltzmann model for solid–liquid phase change," 2013.
[19] R. Yousofvand and K. Ghasemi, "A novel microfluidic device for double emulsion formation: The effects of design parameters on droplet production performance," *Colloids and Surfaces A: Physicochemical and Engineering Aspects*, vol. 635, p. 128059, Feb. 2022.
[20] D. R. Noble and J. R. Torczynski, "A Lattice-Boltzmann Method for Partially Saturated Computational Cells," *International Journal of Modern Physics C*, vol. 9, pp. 1189–1201, Jan. 1998.
[21] O. Bertrand *et al.*, "Melting driven by natural convection A comparison exercise: first results," *International Journal of Thermal Sciences*, vol. 38, no. 1, pp. 5–26, Jan. 1999.